Original Article
Localization of primary prostate cancer: FACBC PET/CT compared with multiparametric MRI using histopathology as reference standard

Knut Håkon Hole[1,2], Andreas Julius Tulipan[2,3], Jeroen Sebastiaan Reijnen[2,4], Eivor Hernes[3], Ljiljana Vlatkovic[5], Agnes Kathrine Lie[5], Mona-Elisabeth Revheim[2,3], Therese Seierstad[6]

[1]Department of Oncologic Radiology, Division of Radiology and Nuclear Medicine, Oslo University Hospital, Radium Hospital, 0424 Oslo, Norway; [2]Institute of Clinical Medicine, University of Oslo, 0359 Oslo, Norway; [3]Department of Nuclear Medicine, Division of Radiology and Nuclear Medicine, Oslo University Hospital, 0424 Oslo, Norway; [4]Department of Radiology, Sørlandet Hospital Trust, 4879 Grimstad, Agder, Norway; [5]Department of Pathology, Oslo University Hospital, 0424 Oslo, Norway; [6]Department of Research and Development, Division of Radiology and Nuclear Medicine, Oslo University Hospital, 0424 Oslo, Norway

Abstract: FACBC (anti-1-amino-3-^{18}F-fluorocyclobutane-1-carboxylic acid) is a FDA-approved PET-tracer in patients with suspected recurrent prostate cancer. In the diagnostic work-up of primary prostate cancer, accurate localization of the index tumor is needed for image-guidance of biopsies. We therefore assessed the performance of FACBC PET/CT to detect and localize the index tumor and compared it to multiparametric MRI (mpMRI) using whole-mount histopathology as reference standard. Twenty-three patients with biopsy-proven prostate cancer had FACBC PET/CT and mpMRI within two weeks prior to prostatectomy. FACBC PET/CT was acquired as 14 minutes list-mode and re-binned into seven 2-minutes intervals. Static FACBC was the acquired data from 4-6 minutes, whereas the dynamic FACBC included all seven intervals. Two radiologists and two nuclear medicine physicians independently interpreted the images and consensus was reached in case of discrepancy. Static PET detected 15 of 23 (65%) of the index tumors, dynamic PET detected 14 of 22 (64%), and MRI detected 20 of 23 (87%). To assess the extent of the tumor, the interpreters delineated the tumor in a 12-regions sector-based template. True positive, true negative, false positive and false negative sectors were recorded based on the template drawings and whole-mount histopathology. Both static and dynamic FACBC PET had sensitivity of 40% and specificity of 99%, whereas MRI had sensitivity of 81% and specificity of 100%. Our data indicate that FACBC PET/CT may be useful but that mpMRI is better for localizing the index tumor in patients with prostate cancer.

Keywords: Prostatic neoplasms, multiparametric magnetic resonance imaging, positron emission tomography, fluciclovine F-18, sensitivity and specificity

Introduction

FACBC (anti-1-amino-3-^{18}F-fluorocyclobutane-1-carboxylic acid) was in May 2016 approved by the U.S. Food and Drug Administration (FDA) as a ^{18}F-labelled positron PET-tracer for use in patients with suspected recurrent prostate cancer (https://www.fda.gov/newsevents/newsroom/pressannouncements/ucm5039-20.htm). In this setting, FACBC has been shown to be superior to ^{11}C-Choline [1], ^{111}In-capromab pendetide single photon emission computerized tomography [2] and computed tomography (CT) [3].

In the diagnostic work-up of prostate cancer, accurate localization of the index tumor is needed for image-guidance of biopsies. Based on the promising results from Turkbey *et al.* who detected 19 of 21 index lesions [4] and the high sensitivity in the study from Schuster *et al.* [5], we set out to investigate the performance of FACBC PET/CT and compare it to mpMRI, which is the commonly used modality to localize the index tumor and target the biopsies in primary prostate cancer.

We have recently shown that there is a strong correlation between the early uptake character-

Table 1. Patient and tumor characteristics

ID	Age [years]	PSA[b] [ng/mL]	Prostate volume [ml]	Pathological T stage[c]	Gleason score
1	70	8.7	52	T3a	9
2	61	9.3	32	T2c	7b
3	58	12.0	39	T3a	7b
4	60	8.7	31	T3a	7b
5	65	8.5	54	T2	6
6	74	4.7	48	T3a	9
7	66	11.0	40	T3a	9
8	68	9.6	38	T2	7a
9	68	5.0	24	T3a	8
10	57	9.1	57	T3a	7a
11	61	8.7	33	T3a	7b
12	58	4.6	44	T2c	7a
13[a]	63	8.2	28	T2c	7b
14	74	12.0	50	T2c	7b
15	66	7.1	42	T3a	7b
16	73	8.3	43	T2c	7a
17	68	37.0	57	T3b	8
18	46	27.0	34	T3a	8
19	71	8.4	58	T2a	6
20	71	16.0	46	T3b	8
21	65	12.0	47	T3a	8
22	67	9.0	36	T3a	7a
23	59	5.4	39	T3a	8

[a], Failed dynamic acquisition; [b], PSA = Prostate Specific Antigen; [c], Local tumor extent according to the TNM classification system (AJCC/UICC 7th edition).

istics of dynamic contrast-enhanced MRI (DCE-MRI) and dynamic FACBC PET [6]. Adding DCE-MRI to morphological imaging has been reported to improve the sensitivity of tumor detection [7, 8] and is included in PI-RADS v2 (Prostate Imaging-Reporting And Data System). In PI-RADS v2 early contrast enhancement increases the suspicion of cancer and upgrades a lesion from PI-RADS 3 to PI-RADS 4 [9]. Therefore, we wanted to investigate if including the early dynamic phase of FACBC PET in addition to the static 4-6 minutes acquisition, recommended by the tracer manufacturer, would translate into improved prostate cancer detection.

The aim of the study was to assess the performance of static and dynamic FACBC PET/CT to detect the index tumor of primary prostate cancer and to compare it to that of multiparametric MRI. We used a cohort of patients referred to prostatectomy, which provides the optimal histopathological reference standard.

Materials and methods

Patient population and study design

This prospective single-institution study (ClinicalTrials.gov NCT01464216) was approved by the institutional review board and the national regional ethics committee (2010/1656), and written informed consent was obtained from all participants. Eligible participants were men with biopsy-proven, intermediate or high-risk prostate cancer referred to prostatectomy. Exclusion criteria were contraindications to MRI or PET/CT or prior cancer treatment. Patient and tumor characteristics of the 23 included patients are shown in **Table 1**. All patients had MRI and PET/CT prior to surgery. The mean number of days between MRI and surgery was 4.4 days (range 0-23) and the mean number of days between PET and surgery was 9.8 days (range 1-18).

MRI

All MRI examinations were performed using a 1.5T General Electric Discovery scanner and a 32 channels phased array coil. The MRI examination was performed for TNM-staging and consisted of anatomical T1- and T2-weighed sequences covering the pelvis and the lower abdomen, and functional imaging (DWI and DCE-MRI) of the prostate region in line with the technical recommendations of PI-RADS [10]. The MRI sequences and acquisition parameters are summarized in Supplementary Table 1. The patients were given laxative to empty the rectum one hour prior to MRI. Peristalsis was suppressed by intravenous administration of 1 mg butyl scopolamine (Buscopan®, Boehringer Ingelheim, Germany) and intramuscular administration of 1 mg glucagon (Novo Nordisk, Bagsværd, Denmark). Two experienced radiologists (KHH and JSR, 11 and 10 years of prostate MRI experience) independently assessed the MRI images and the localization and extent of the index lesion were drawn on template schematic of the prostate gland and the vesicles [11]. The interpretation of the multiparametric MRI (mpMRI) examination was based on the guidelines presented in the first version of PI-RADS [10]. The readers knew that the patients had cancer but were blinded to the results from PET/CT and preoperative histopa-

thology. In three cases of discordant findings, consensus was reached.

FACBC PET/CT

All FACBC PET/CT examinations were acquired using a Biograph40 mCT PET/CT (Siemens, Erlangen, Germany). The patients fasted for at least four hours and voided the bladder before the examination. A helical CT scan of the pelvis for attenuation correction was followed by an intravenous bolus administration of 281-301 MBq FACBC (MAPP Medical Technologies, Tikkakoski, Finland and Norwegian Medical Cyclotron Centre, Oslo, Norway) and saline flush of 10-20 ml. A 14-minutes list-mode PET acquisition of one bed position (axial field of view (FOV) of 21.6 cm centered above the symphysis, FOV of the PET ring diameter 70 cm) was started before administration of FACBC. The list-mode data was reconstructed into 7 image time frames of 2 minutes each. The images were reconstructed using 3D iterative ordered-subset expectation maximization (OSEM) with two iterations and 21 subsets, time of flight (TOF), point-spread function (PSF)-correction, slice thickness 1.5 mm, matrix size 200×200, and a Gaussian post-reconstruction convolution kernel with full width at half maximum (FWHM) of three millimeters. Two experienced nuclear medicine physicians (MER and EH, 14 and 7 years of PET experience, respectively) independently interpreted the FACBC PET/CT images using the SyngoVia software. A combination of maximum intensity projections (MIPs), PET, CT and fused PET/CT were used. Without existing guidelines for interpretation, PET was interpreted as positive where tracer uptake was higher than the background prostate tissue, also taken into account typical localizations, uptake pattern, and the possibility of benign hyperplasia. First, the static FACBC PET/CT images acquired 4-6 minutes after FACBC administration was reviewed. The localization and extent of the lesions were drawn on the template [11]. Next, the additional 2-minutes intervals (0-2, 2-4, 6-8, 8-10, 10-12, and 12-14 minutes) were separately interpretated and a second drawing of tumor location and extent was recorded. The readers knew that the patients had cancer, but were blinded to other imaging, clinical and histopathological findings. After each nuclear medicine physicians individually had interpreted all FACBC PET/CT exams, a consensus meeting was held in order to decide on a common PET report.

Robot-assisted laparoscopic prostatectomy

Robot-assisted laparoscopic prostatectomy was performed with a three-armed robotic DaVinci® system (Intuitive Surgical, Sunnyvale, CA, USA) and a surgical approach based on the Vattikutti Institute technique [12]. The entire prostate and seminal vesicles were removed.

Histopathology

The resected prostate gland was coated with three different inks and fixed in 10% buffered formaldehyde for at least two days. Gross sectioning was performed according to a standardized protocol where total prostate with seminal vesicles were embedded in paraffin blocks [13, 14]: The apex and base of the prostate as sagittal sections with the cone method. The remaining body was sectioned serially at 3-4 mm intervals in the transverse plane and prepared as whole-mount sections. 5 μm hematoxylin and eosin (HE)-stained sections from each block were examined by one of two experienced uropathologists (LV and AKL). All individual tumor foci were outlined in the sections. T-classification was recorded according to AJCC/UICC 7th edition and Gleason graded according to the update on the Gleason grading system [15]. The index lesion was defined, in descending order, by T-stage, Gleason score, and largest diameter [16]. Tumor was drawn using the same template as for imaging [11].

Data analyses

For data analyses the 27-regions of interest template was reduced to 12 sectors. The location of the index tumor was coded into three levels (apex, mid, base) and four quadrants (anterior, posterior, right, left). A consensus meeting including radiologist and nuclear medicine physicians was held to define true positive, true negative, false negative and false positive sectors. More than one sector was defined as positive if (I) the drawing of the index tumor occupied more than 1/3 of a neighboring sector(s) or (II) more than 1/3 of the index tumor extended into neighboring sector(s) as illustrated in **Figure 1**. Because the aim was to localize the index tumors, correctly localized non-index tumors were considered as true negatives in the analyses. If discordance between
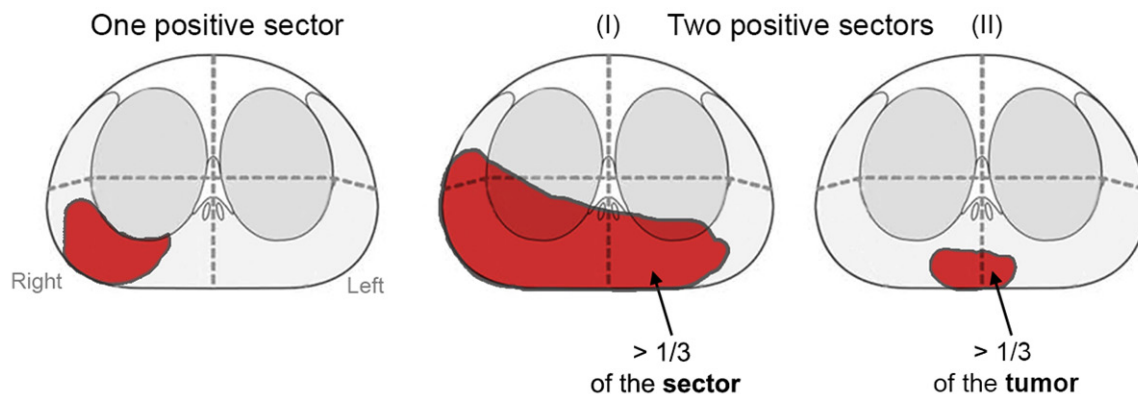
Figure 1. Definition of positive sectors. If a tumor extends beyond one sector we defined the neighboring sector(s) as positive in two situations: (I) The tumor occupies more than one third of the neighboring sector. (II) More than one third of the tumor extends into the neighboring sector. E.g. the right upper sector in (I) contains tumor but is negative because it does not fulfill any of these two criteria.
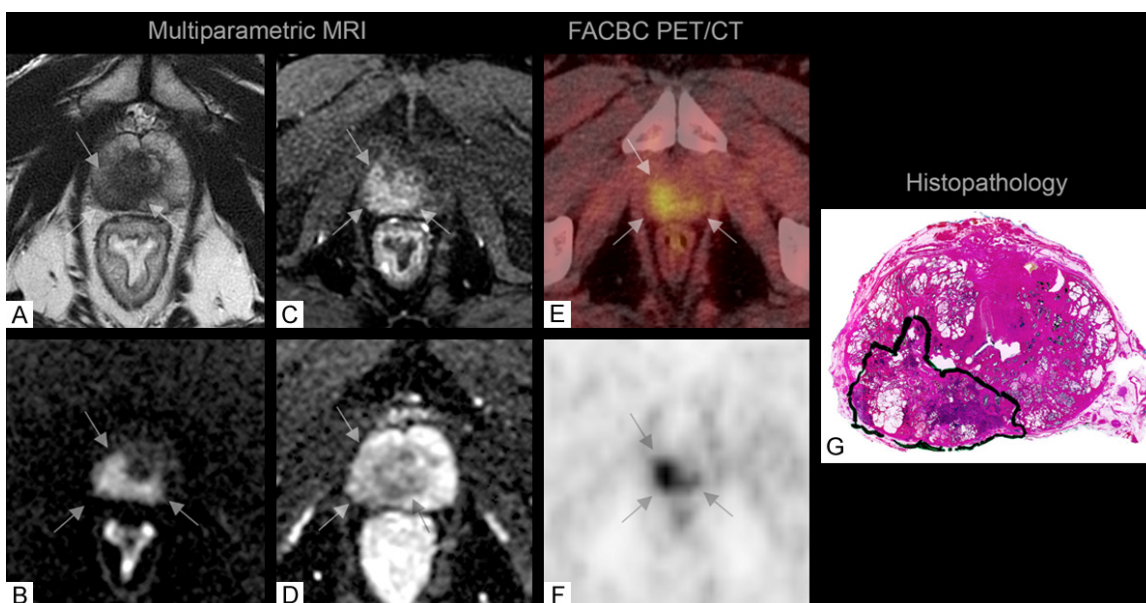
Figure 2. Concordant image findings at MRI and FACBC PET/CT of a 60-year-old man with a T3a Gleason score 4+3 tumor located posteriorly in the right side of the prostate (arrows). Axial MRI images: T2W (A), DWI b1400 (B), early enhancement DCE (C) and ADC (D). Axial FACBC images: Fused FACBC PET/CT (E) and attenuated-corrected FACBC PET (F). Corresponding whole-mount H&E stained prostatectomy specimen with the tumor borders drawn in black ink (G).

the template drawings from MRI, PET and histopathology, the pathologist's outlining on the HE slides were used as reference. We investigated both if the index tumor was detected, and if the extent of the index tumor was recognized. The performance was compared by calculating sensitivity and specificity.

Results

Figure 2 shows the PET and MRI images of a patient with concordant findings at imaging and histopathology. All seven time frames from the dynamic PET acquisition are shown in Supplementary Figure 1. The corresponding schematic drawings are shown in **Figure 3**. **Figure 4** shows two discordant cases, one without pathologic FACBC uptake in the tumor and one where the uptake in tumor could not be differentiated from high uptake in benign tissue.

Static $PET_{4\text{-}6\ min}$ detected 15 of 23 (65%) of the index tumors, dynamic $PET_{7\times2\ min}$ detected 14 of 22 (64%), and MRI detected 20 of 23 (87%).
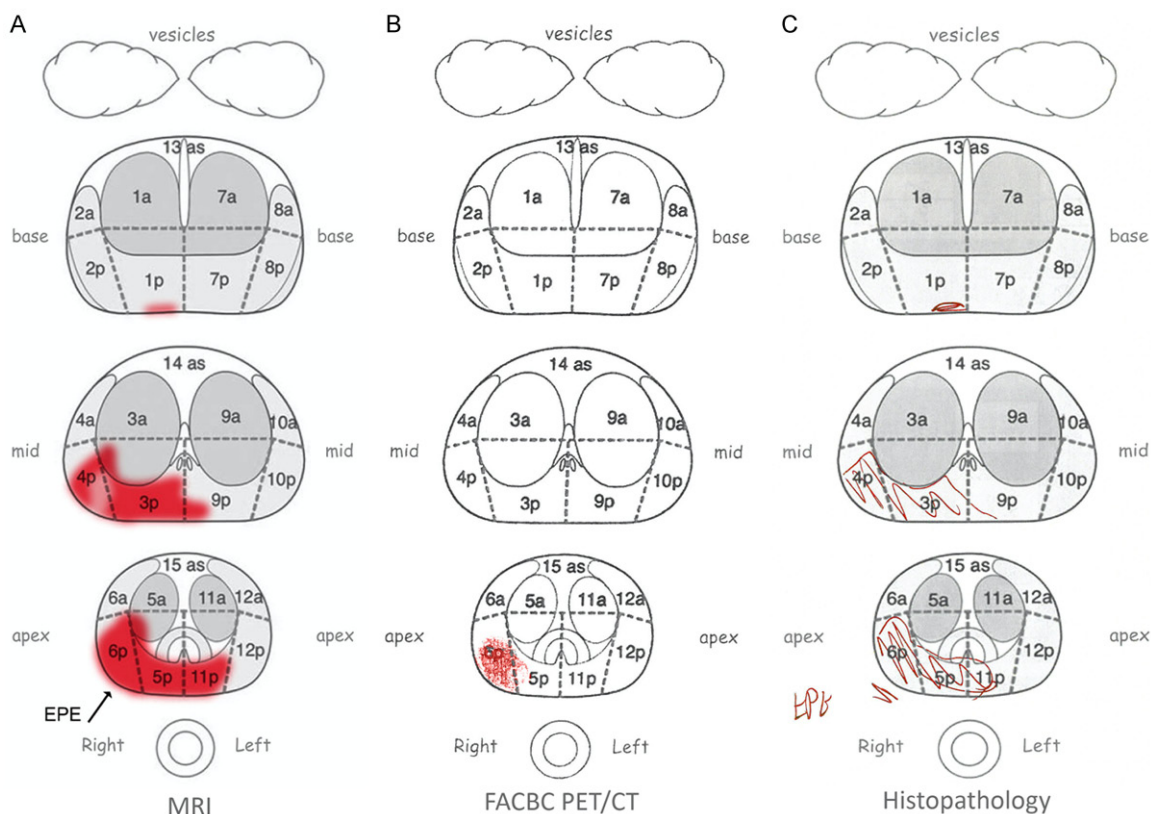
Figure 3. The original schematic drawings of the tumor extent of the patient in **Figure 2**. Digitally painted by the radiologist (A). Hand-drawn by the nuclear medicine physician (B) and the pathologist (C). This is an example where the nuclear medicine physician correctly localized the index tumor but underestimated the extent of the tumor. Extraprostatic extension (EPE) was detected by the radiologist (arrow) and confirmed by the pathologist ("EPE" in handwriting).

Seven index tumors were missed at both static and dynamic PET. One index tumor was detected at static PET only (ID 6) and one at dynamic PET only (ID 17). Three index tumors were missed at MRI, of which one was detected at PET (ID 19).

In the sector-based analyses static $PET_{4-6\ min}$ detected 23 of 57 (40%) of the index tumor positive sectors, dynamic $PET_{7\times2\ min}$ detected 22 of 55 (40%), and MRI detected 46 of 57 (80%). The results from the sector-based analyses are summarized in **Table 2** and presented for individual patients in Supplementary Tables 2, 3, 4.

Discussion

In this study of 23 patients with primary prostate cancer, we found that FACBC PET/CT had high specificity, but lower sensitivity compared to multiparametric MRI for localization of the index tumor. Furthermore, dynamic acquisition did not improve the performance of FACBC PET/CT. PET detected 65% of the index tumors. In the sector-based analyses, PET correctly localized 23 of the 57 positive sectors and 217 of the 219 negative sectors, which gives sensitivity of 40% and specificity of 99%.

We have found four other studies that have investigated FACBC PET/CT for localization of tumor in a cohort of patients with known prostate cancer [4, 5, 17, 18]. In line with our study, all four had sector-based assessment and histopathology as reference standard, which makes them relevant for comparison. Jambor et al. used 12-regions sector-based analyses in 26 patient and found higher sensitivity (87%) and lower specificity (56%) [17]. One explanation, as stated by the authors, was that high FACBC uptake in benign hyperplasia was categorized as positive sectors. Turkbey et al. used 20-regions sector-based analyses in 21 pati-
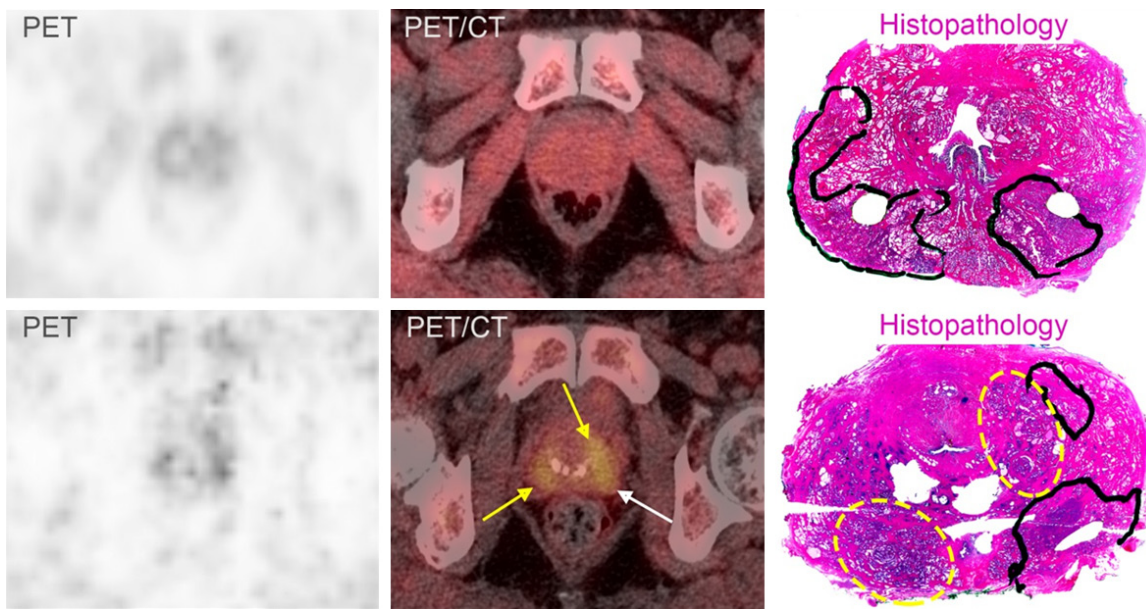
Figure 4. Discordant image findings at FACBC PET/CT. Upper row: A 58-year-old man with a Gleason score 3+4 tumor located posteriolaterally on the right side and a Gleason 3+3 tumor located posteriorly on the left side. The FACBC uptake was low and uniform in the entire prostate, both in the tumor and in the benign tissue. Lower row: A 66-year-old man with a Gleason score 4+3 tumor located posteriorly on the left side and a small Gleason 3+3 tumor located anteriorly. The FACBC uptake in the index tumor (white arrow) could not be differentiated from the uptake in benign cellular tissue (yellow arrows and circles).

Table 2. Diagnostic performance using sector-based analysis of all index tumors

	FACBC PET$_{4\text{-}6\ min}$	FACBC PET$_{7\times2\ min}$	Multiparametric MRI
True Positives	23	22	46
True Negatives	217	206	219
False Positives	2	3	0
False Negatives	34	33	11
Sectors (N)	276	264[a]	276
Sensitivity (%)	40.4	40.0	80.7
Specificity (%)	99.1	98.6	100

[a], dynamic acquisition failed for one patient.

ents and found higher sensitivity (67%) and lower specificity (66%) [4]. Similar to Jambor *et al.* they included not only the index tumor, which may contribute to the different results from ours. In addition, Turkbey *et al.* reported that FACBC PET/CT localized 90% of the dominant tumors, whereas we localized 65%. Schuster *et al.* used 12-regions sector-based analyses in 10 patients and found much higher sensitivity (80-90%) and much lower specificity (18-50%) [5], indicating that they used a lower cut-off for interpretation of pathological uptake. The main aim of their study, however, was to investigate

optimal timepoint and establish a cut-off value for SUVmax. They set out to determine if FACBC uptake correlated with presence or absence of tumor but found substantial overlap between malignant and non-malignant tissue. Suzuki *et al.* used 6-regions sector-based analyses in 43 patients and found clearly higher sensitivity (93%) and slightly lower specificity (90%) [18]. Probable explanations for the high sensitivity, as stated by the authors, are that they divided the prostate into fewer segments, almost all were high-risk patients, and that the primary lesions were large.

Only two of the four studies compared the performance of FACBC PET/CT with MRI [4, 17]. In our study mpMRI detected 87% of the index tumors. In the sector-based analyses, mpMRI correctly localized 46 of the 57 positive sectors and there were no false positive sectors, which gives sensitivity of 81% and specificity of 100%. Our results are in accordance with the two other studies. Jambor *et al.* found substantially higher specificity of mpMRI (99%) compared to

FACBC (56%), and the sensitivity of PET was significantly improved (96%) by adding MRI to the interpretation (FACBC PET/MR) [17]. Turkbey *et al.* reported their results for each of the MRI sequences separately, and not as a multiparametric interpretation as in PI-RADS. Nevertheless, the performance of T2-weighted imaging and apparent diffusion coefficient maps was better than FACBC [4].

In the diagnostic work-up of patients with suspected prostate cancer it is important to reliably detect clinically significant cancers, and at the same time avoid unnecessary biopsies and avoid diagnosing clinically insignificant cancer [19]. High sensitivity as well as high specificity is required. In FACBC PET, defining the cut-off for pathological uptake seems to be a trade-off between false positives and false negatives. The varying results from the different studies illustrate this challenge: We obtained high specificity (99%) at the expense of sensitivity (40%), whereas Jambor *et al.* obtained high sensitivity (87%) at the expense of specificity (56%) [17]. The varying results indicate that a defined cut-off for pathological uptake and guidelines on interpretation of FACBC PET are needed, such as PI-RADS for mpMRI. Therefore, the current potential use of FACBC in the work-up of patients with suspected prostate cancer seems to be limited to situations when mpMRI is unavailable or contraindicated. However, in such cases other tracers such as prostate-specific membrane antigen (PSMA) may also be considered.

Our study had strengths and limitations. All patients had MRI and PET shortly prior to prostatectomy, which is the optimal reference standard, and experienced readers interpreted the examinations independently. Thus, the study design is well suited for comparison of the modalities. However, the number of patients is limited, considering the biologically heterogeneity of the disease. In lack of established threshold for pathological FACBC uptake, the interpretation was qualitative. Furthermore, our study cohort, similarly to the four other studies, consisted of patients with histologically confirmed prostate cancer and relatively high Gleason score. Therefore, the results may not be transferable to cohorts of biopsy-naïve patients.

In conclusion, in this study of 23 patients, we found that FACBC PET/CT had high specificity but limited sensitivity for localization of the index tumor in primary prostate cancer. Multiparametric MRI performed better than FACBC PET/CT. Dynamic acquisition did not improve the performance of FACBC PET/CT.

Disclosure of conflict of interest

None.

Address correspondence to: Therese Seierstad, Department of Research and Development, Division of Radiology and Nuclear Medicine, Oslo University Hospital, P. O. box 4953, Nydalen, 0424 Oslo, Norway. Tel: +47-46451987; E-mail: therese@radium.uio.no

References

[1] Nanni C, Zanoni L, Pultrone C, Schiavina R, Brunocilla E, Lodi F, Malizia C, Ferrari M, Rigatti P, Fonti C, Martorana G and Fanti S. (18)F-FACBC (anti1-amino-3-(18)F-fluorocyclobutane-1-carboxylic acid) versus (11)C-choline PET/CT in prostate cancer relapse: results of a prospective trial. Eur J Nucl Med Mol Imaging 2016; 43: 1601-1610.

[2] Schuster DM, Nieh PT, Jani AB, Amzat R, Bowman FD, Halkar RK, Master VA, Nye JA, Odewole OA, Osunkoya AO, Savir-Baruch B, Alaei-Taleghani P and Goodman MM. Anti-3-[(18)F]FACBC positron emission tomography-computerized tomography and (111)In-capromab pendetide single photon emission computerized tomography-computerized tomography for recurrent prostate carcinoma: results of a prospective clinical trial. J Urol 2014; 191: 1446-1453.

[3] Odewole OA, Tade FI, Nieh PT, Savir-Baruch B, Jani AB, Master VA, Rossi PJ, Halkar RK, Osunkoya AO, Akin-Akintayo O, Zhang C, Chen Z, Goodman MM and Schuster DM. Recurrent prostate cancer detection with anti-3-[(18)F]FACBC PET/CT: comparison with CT. Eur J Nucl Med Mol Imaging 2016; 43: 1773-1783.

[4] Turkbey B, Mena E, Shih J, Pinto PA, Merino MJ, Lindenberg ML, Bernardo M, McKinney YL, Adler S, Owenius R, Choyke PL and Kurdziel KA. Localized prostate cancer detection with 18F FACBC PET/CT: comparison with MR imaging and histopathologic analysis. Radiology 2014; 270: 849-856.

[5] Schuster DM, Taleghani PA, Nieh PT, Master VA, Amzat R, Savir-Baruch B, Halkar RK, Fox T, Osunkoya AO, Moreno CS, Nye JA, Yu W, Fei B, Wang Z, Chen Z and Goodman MM. Characterization of primary prostate carcinoma by anti-1-amino-2-[(18)F] -fluorocyclobutane-1-carboxylic acid (anti-3-[(18)F] FACBC) uptake. Am J Nucl Med Mol Imaging 2013; 3: 85-96.

[6] Tulipan AJ, Vlatkovic L, Malinen E, Brennhovd B, Hole KH, Lie AK, Ragnum HB, Revheim ME and Seierstad T. Comparison of time curves from dynamic ^{18}F-fluciclovine positron emission tomography and dynamic contrast-enhanced magnetic resonance imaging for primary prostate carcinomas. Phys Imaging Radiat Oncol 2018; 7: 51-57.

[7] Sun C, Chatterjee A, Yousuf A, Antic T, Eggener S, Karczmar GS and Oto A. Comparison of T2-weighted imaging, DWI, and dynamic contrast-enhanced mri for calculation of prostate cancer index lesion volume: correlation with whole-mount pathology. AJR Am J Roentgenol 2019; 212: 351-356.

[8] Taghipour M, Ziaei A, Alessandrino F, Hassanzadeh E, Harisinghani M, Vangel M, Tempany CM and Fennessy FM. Investigating the role of DCE-MRI, over T2 and DWI, in accurate PI-RADS v2 assessment of clinically significant peripheral zone prostate lesions as defined at radical prostatectomy. Abdom Radiol (NY) 2019; 44: 1520-1527.

[9] Weinreb JC, Barentsz JO, Choyke PL, Cornud F, Haider MA, Macura KJ, Margolis D, Schnall MD, Shtern F, Tempany CM, Thoeny HC and Verma S. PI-RADS prostate imaging-reporting and data system: 2015, version 2. Eur Urol 2016; 69: 16-40.

[10] Barentsz JO, Richenberg J, Clements R, Choyke P, Verma S, Villeirs G, Rouviere O, Logager V and Fütterer JJ; European Society of Urogenital Radiology. ESUR prostate MR guidelines 2012. Eur Radiol 2012; 22: 746-757.

[11] Dickinson L, Ahmed HU, Allen C, Barentsz JO, Carey B, Futterer JJ, Heijmink SW, Hoskin PJ, Kirkham A, Padhani AR, Persad R, Puech P, Punwani S, Sohaib AS, Tombal B, Villers A, van der Meulen J and Emberton M. Magnetic resonance imaging for the detection, localisation, and characterisation of prostate cancer: recommendations from a European consensus meeting. Eur Urol 2011; 59: 477-494.

[12] Menon M, Shrivastava A, Kaul S, Badani KK, Fumo M, Bhandari M and Peabody JO. Vattikuti Institute prostatectomy: contemporary technique and analysis of results. Eur Urol 2007; 51: 648-657; discussion 657-648.

[13] Epstein JI, Amin M, Boccon-Gibod L, Egevad L, Humphrey PA, Mikuz G, Newling D, Nilsson S, Sakr W, Srigley JR, Wheeler TM and Montironi R. Prognostic factors and reporting of prostate carcinoma in radical prostatectomy and pelvic lymphadenectomy specimens. Scand J Urol Nephrol Suppl 2005; 34-63.

[14] Srigley JR. Key issues in handling and reporting radical prostatectomy specimens. Arch Pathol Lab Med 2006; 130: 303-317.

[15] Epstein JI. Update on the Gleason grading system. Ann Pathol 2011; 31 Suppl: S20-26.

[16] Samaratunga H, Montironi R, True L, Epstein JI, Griffiths DF, Humphrey PA, van der Kwast T, Wheeler TM, Srigley JR, Delahunt B and Egevad L; ISUP Prostate Cancer Group. International Society of Urological Pathology (ISUP) consensus conference on handling and staging of radical prostatectomy specimens. Working group 1: specimen handling. Mod Pathol 2011; 24: 6-15.

[17] Jambor I, Kuisma A, Kähkönen E, Kemppainen J, Merisaari H, Eskola O, Teuho J, Perez IM, Pesola M, Aronen HJ, Boström PJ, Taimen P and Minn H. Prospective evaluation of (18)F-FACBC PET/CT and PET/MRI versus multiparametric MRI in intermediate- to high-risk prostate cancer patients (FLUCIPRO trial). Eur J Nucl Med Mol Imaging 2018; 45: 355-364.

[18] Suzuki H, Inoue Y, Fujimoto H, Yonese J, Tanabe K, Fukasawa S, Inoue T, Saito S, Ueno M and Otaka A. Diagnostic performance and safety of NMK36 (trans-1-amino-3-[18F]fluoro-cyclobutanecarboxylic acid)-PET/CT in primary prostate cancer: multicenter Phase IIb clinical trial. Jpn J Clin Oncol 2016; 46: 152-162.

[19] Padhani AR, Barentsz J, Villeirs G, Rosenkrantz AB, Margolis DJ, Turkbey B, Thoeny HC, Cornud F, Haider MA, Macura KJ, Tempany CM, Verma S and Weinreb JC. PI-RADS steering committee: the PI-RADS multiparametric MRI and MRI-directed biopsy pathway. Radiology 2019; 292: 464-474.

Supplementary Table 1. The MRI protocol and acquisition parameters

Acquisition parameters	T2W FSE	ADC	DWI	T2W CUBE	T1W CUBE	DCE	T1W post Gd
Pulse sequence	2D SE	SE-EPI	SE-EPI	3D SE	3D SE	3D Spoiled GE-Dixon	3D Spoiled GE-Dixon
Acquisition plane	sagittal/transversal/coronal	transversal	transversal	transversal	coronal	transversal	coronal
Echo time (ms)	99	59	64	89	8.0	3.1	3.6
Repetition time (ms)	3376/2954/2954	3000	6000	1200	400	5.8	7.9
Flip anlge	90	90	90	variable	variable	15	15
Slice thickness							
Acquired	3	4	4	1	2	2.6	2.0
Interpolated					1		
Slice gap	1	1	1	0	0	0	0
Number of excitations	6	2	16	2	1	1	1
Inplane resolution (mm × mm)							
Acquired	0.56×0.56	1.96×1.96	1.96×1.96	1.00×1.00	1.20×1.20	1.50×1.50	1.00×1.00
Interpolated	0.35×0.35	0.70×0.70	0.70×0.70	0.63×0.63	0.90×0.90	0.94×0.94	0.86×0.86
Echo train	28	92	92	90	30		1
Bandwidth (Hz/pixel)	325	1953	1953	488	488		325
FOV (mm × mm)	180×180	180×180	180×180	320×320	460×460	240×240	440×440
Matrix size (pixels × pixels)							
Acquired	320×320	92×92	92×92	320×320	384×384	160×160	440×440
Interpolated	512×512	256×256	256×256	512×512	512×512	256×256	512×512
Parallell imaging factor	2	1	1	2.5×2	2×2	2	3×2
Motion correction	PROPELLER	no	no	no	no	yes[*]	no
b-values (s/mm^2)	NA	0-100-200-300-400-500-600-700-800-900-1000	1500	NA	NA	NA	NA
Time resolution (sec)	NA	NA	NA	NA	NA	11.4	NA
Acquisition time	4:37/4:02/4:02	4:09	6:30	7:33	2:56	5:43	1:13

ADC: Apparent Diffusion Coefficient; DCE: dynamic contrast-enhanced; Diffusion-Weighted Imaging: EPI: echo planar imaging; FSE: Fast Spin Echo; FOV: field of view; MR: Magnetic Resonance; T2W: T2 weighted; DWI: PROPELLER: Periodically Rotated Overlapping ParallEL Lines with Enhanced Reconstruction; SE: spin echo; GE: gradient echo. [*], performed using nICE (Nordic Neurolab, Bergen, Norway).
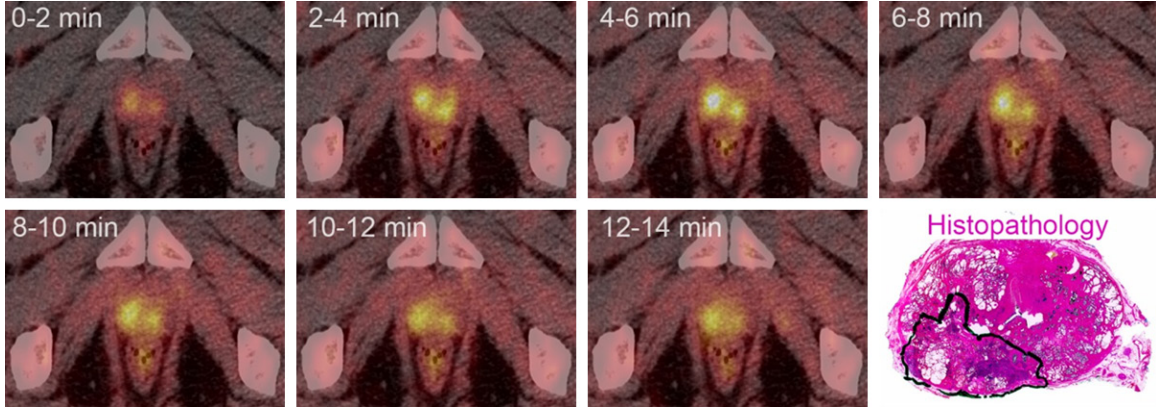
Supplementary Figure 1. Dynamic FACBC PET/CT images for the seven 2-minutes time frames of the patient in **Figure 2**. Gleason score 4+3 tumor located posteriorly in the right side of the prostate. Corresponding whole-mount H&E stained prostatectomy specimen with the tumor borders drawn in black ink. Notably, the FACBC uptake seems to be more prominent in benign tissue at the earliest time points and more prominent in tumor at later time points.

Supplementary Table 2. Performance of static FACBC PET/CT$_{4-6\,min}$ for detection of the extent of the index tumor in primary prostate cancer

	Index tumor at H&E			Localization of index tumor at static FACBC PET/CT															
ID	d1 (mm)	d2 (mm)	Gleason grade	BRA	BRP	BLA	BLP	MRA	MRP	MLA	MLP	ARA	ARP	ALA	ALP	TP	TN	FP	FN
1	18	9	4+4	TN	TN	TN	TN	TN	TN	TN	TP	TN	TN	TN	TN	1	11	0	0
2	23	10	4+3	TN	TN	TN	TN	TN	TN	TP	TN	TN	TN	TN	TN	1	11	0	0
3	20	15	7b	TN	TP	TN	TN	TN	TN	TN	TN	TN	TN	TN	TN	1	11	0	0
4	32	21	7b	TN	FN	TN	TN	TN	TP	TN	TN	TN	TP	TN	FN	2	8	0	2
5	12	7	3+3	TN	TN	TN	TN	TN	TN	FN	TN	TN	TN	FN	TN	0	10	0	2
6	33	18	4+5	TN	FN	TN	TN	TP	TP	TN	TN	FN	TP	TN	TN	3	7	0	2
7	29	12	4+5	TN	FN	TN	TN	TN	TP	TN	TN	TN	TN	TN	TN	1	10	0	1
8	22	15	3+4	TN	TN	TN	TN	FN	TN	FN	TN	FN	TN	TN	TN	0	9	0	3
9	25	13	4+4	TN	TN	TN	TP	TN	TN	TN	TP	TN	TN	TN	TN	2	10	0	0
10	29	18	3+4	TN	TN	TN	TN	TN	FN	TN	TN	TN	FN	TN	TN	0	10	0	2
11	22	16	4+3	TN	TN	TN	TN	TN	TN	TN	TP	TN	TN	TN	FN	1	10	0	1
12	15	13	3+4	TN	TN	TN	FN	TN	TN	TN	FN	TN	TN	TN	TN	0	10	0	2
13	18	11	4+3	TN	TN	TN	TN	TN	FN	TN	TN	TN	TP	TN	TN	1	10	0	1
14	17	5	4+3	TN	TN	TN	TN	FN	TN	TN	TN	TN	TN	TN	TN	0	11	0	1
15	20	12	4+3	TN	TN	TN	FN	TN	TN	TN	FN	TN	TN	TN	TN	0	10	0	2
16	33	20	3+4	TN	TN	TN	TN	TP	TN	FN	TN	FN	TN	TP	TN	2	8	0	2
17	37	8	4+4	TN	TN	TN	TN	TN	FN	TN	FN	TN	FN	TN	FN	0	8	0	4
18	25	16	4+4	TN	TP	TN	TN	FP	TP	TN	TN	TN	TN	TN	TN	2	9	1	0
19	14	7	3+3	TN	TN	TN	TN	TN	TN	TP	TN	FN	TN	TP	FP	2	8	1	1
20	35	10	4+4	TN	TN	TN	FN	TN	TN	TN	TP	TN	TN	TN	TN	1	10	0	1
21	33	25	4+4	TN	TN	TN	FN	TN	TN	TN	TP	TN	FN	TN	TP	2	8	0	2
22	30	25	3+4	FN	FN	TN	TN	FN	FN	TN	TN	TN	TN	TN	TN	0	8	0	4
23	13	6	4+4	TN	FN	TN	TN	TP	TN	TN	TN	TN	TN	TN	TN	1	10	0	1

H&E = Hematoxylin and Eosin, BRA = basis right lobe anterior, BRP = basis right lobe posterior, BLA = basis left lobe anterior, BLP = basis left lobe posterior, MRA = mid right lobe anterior, MRP = mid right lobe posterior, MLA = mid left lobe anterior, MLP = mid left lobe posterior, ARA = apex right lobe anterior, ARP = apex right lobe posterior, ALA = apex left lobe anterior, ALP = apex left lobe posterior, TP = true positive, TN = true negative, FP = false positive, FN = false negative.

Supplementary Table 3. Performance of dynamic FACBC PET/CT$_{7\times2\ min}$ for detection of the extent of the index tumor in primary prostate cancer

	Index tumor at H&E			Localization of index tumor at dynamic FACBC PET/CT															
ID	d1 (mm)	d2 (mm)	Gleason grade	BRA	BRP	BLA	BLP	MRA	MRP	MLA	MLP	ARA	ARP	ALA	ALP	TP	TN	FP	FN
1	18	9	4+5	TN	TN	TN	TN	TN	TN	TN	TP	TN	TN	TN	TN	1	11	0	0
2	23	10	4+3	TN	TN	TN	TN	TN	TN	TP	TN	TN	TN	TN	TN	1	11	0	0
3	20	15	7b	TN	TP	TN	TN	TN	TN	TN	TN	TN	TN	TN	TN	1	11	0	0
4	32	21	7b	TN	FN	TN	TN	TN	TP	TN	TN	TN	TP	TN	TP	3	8	0	1
5	12	7	3+3	TN	TN	TN	TN	TN	TN	FN	TN	TN	TN	FN	TN	0	10	0	2
6	33	18	4+5	TN	FN	TN	TN	FN	FN	TN	TN	FN	FN	TN	TN	0	7	0	5
7	29	12	4+5	TN	FN	TN	TN	TN	TP	TN	TN	TN	TN	TN	TN	1	10	0	1
8	22	15	3+4	TN	TN	TN	TN	FN	TN	FN	TN	FN	TN	TN	TN	0	9	0	3
9	25	13	4+4	TN	TN	TN	TP	TN	TN	TN	TP	TN	TN	TN	TN	2	10	0	0
10	29	18	3+4	TN	TN	TN	TN	TN	FN	TN	TN	TN	FN	TN	TN	0	10	0	2
11	22	16	4+3	TN	TN	TN	TN	TN	TN	TN	TP	TN	TN	TN	TP	2	10	0	0
12	15	13	3+4	TN	TN	TN	FN	TN	TN	TN	FN	TN	TN	TN	TN	0	10	0	2
13	18	11	4+3																
14	17	5	4+3	TN	TN	TN	TN	FN	TN	TN	TN	TN	FP	TN	TN	0	10	1	1
15	20	12	4+3	TN	TN	TN	FN	TN	TN	TN	FN	TN	TN	TN	TN	0	10	0	2
16	33	20	3+4	TN	TN	TN	TN	TP	TN	FN	TN	FN	TN	TP	TN	2	8	0	2
17	37	8	4+4	TN	TN	TN	TN	TN	FN	TN	TP	TN	FN	TN	TP	2	8	0	2
18	25	16	4+4	TN	TP	TN	TN	FP	TP	TN	TN	TN	TN	TN	TN	2	9	1	0
19	14	7	3+3	TN	TN	TN	TN	TN	TN	FN	TN	FN	TN	TP	FP	1	8	1	2
20	35	10	4+4	TN	TN	TN	FN	TN	TN	TN	TP	TN	TN	TN	TN	1	10	0	1
21	33	25	4+4	TN	TN	TN	FN	TN	TN	TN	TP	TN	FN	TN	TP	2	8	0	2
22	30	25	3+4	FN	FN	TN	TN	FN	FN	TN	TN	TN	TN	TN	TN	0	8	0	4
23	13	6	4+4	TN	FN	TN	TN	TP	TN	TN	TN	TN	TN	TN	TN	1	10	0	1

H&E = Hematoxylin and Eosin, BRA= basis right lobe anterior, BRP= basis right lobe posterior, BLA = basis left lobe anterior, BLP = basis left lobe posterior, MRA = mid right lobe anterior, MRP = mid right lobe posterior, MLA = mid left lobe anterior, MLP = mid left lobe posterior, ARA = apex right lobe anterior, ARP = apex right lobe posterior, ALA = apex left lobe anterior, ALP = apex left lobe posterior, TP = true positive, TN = true negative, FP = false positive, FN = false negative.

Supplementary Table 4. Performance of multiparametric MRI for detection of the extent of the index tumor in primary prostate cancer

	Index tumor at H&E			Localization of index tumor at multiparametric MRI															
ID	d1 (mm)	d2 (mm)	Gleason grade	BRA	BRP	BLA	BLP	MRA	MRP	MLA	MLP	ARA	ARP	ALA	ALP	TP	TN	FP	FN
1	18	9	4+4	TN	TN	TN	TN	TN	TN	TN	TP	TN	TN	TN	TN	1	11	0	0
2	23	10	4+3	TN	TN	TN	TN	TN	TN	TP	TN	TN	TN	TN	TN	1	11	0	0
3	20	15	7b	TN	TP	TN	TN	TN	TN	TN	TN	TN	TN	TN	TN	1	11	0	0
4	32	21	7b	TN	TP	TN	TN	TP	TN	TN	TN	TN	TP	TN	TP	4	8	0	0
5	12	7	3+3	TN	TN	TN	TN	TN	TN	FN	TN	TN	TN	FN	TN	0	10	0	2
6	33	18	4+5	TN	TP	TN	TN	TP	TP	TN	TN	TP	TP	TN	TN	5	7	0	0
7	29	12	4+5	TN	TP	TN	TN	TN	TP	TN	TN	TN	TN	TN	TN	2	10	0	0
8	22	15	3+4	TN	TN	TN	TN	TP	TN	TP	TN	TP	TN	TN	TN	3	9	0	0
9	25	13	4+4	TN	TN	TN	TP	TN	TN	TN	TP	TN	TN	TN	TN	2	10	0	0
10	29	18	3+4	TN	TN	TN	TN	TN	TP	TN	TN	TN	FN	TN	TN	1	10	0	1
11	22	16	4+3	TN	TN	TN	TN	TN	TN	TN	TP	TN	TN	TN	TP	2	10	0	0
12	15	13	3+4	TN	TN	TN	TN	TN	TN	TN	FN	TN	TN	TN	TP	1	10	0	1
13	18	11	4+3	TN	TN	TN	TN	TN	FN	TN	TN	TN	TP	TN	TN	1	10	0	1
14	17	5	4+3	TN	TN	TN	TN	FN	TN	TN	TN	TN	TN	TN	TN	0	11	0	1
15	20	12	4+3	TN	TN	TN	TP	TN	TN	TN	TP	TN	TN	TN	TN	2	10	0	0
16	33	20	3+4	TN	TN	TN	TN	FN	TN	TP	TN	TP	TN	TP	TN	3	8	0	1
17	37	8	4+4	TN	TN	TN	TN	TN	TP	TN	TP	TN	TP	TN	TP	4	8	0	0
18	25	16	4+4	TN	TP	TN	TN	TN	TP	TN	TN	TN	TN	TN	TN	2	10	0	0
19	14	7	3+3	TN	TN	TN	TN	TN	TN	FN	TN	FN	TN	FN	TN	0	9	0	3
20	35	10	4+4	TN	TN	TN	TP	TN	TN	TN	TP	TN	TN	TN	TN	2	10	0	0
21	33	25	4+4	TN	TN	TN	TP	TN	TN	TN	TP	TN	FN	TN	TP	3	8	0	1
22	30	25	3+4	TP	TP	TN	TN	TP	TP	TN	TN	TN	TN	TN	TN	4	8	0	0
23	13	6	4+4	TN	TP	TN	TN	TN	TP	TN	TN	TN	TN	TN	TN	2	10	0	0

H&E = Hematoxylin and Eosin, BRA = basis right lobe anterior, BRP = basis right lobe posterior, BLA = basis left lobe anterior, BLP = basis left lobe posterior, MRA = mid right lobe anterior, MRP = mid right lobe posterior, MLA = mid left lobe anterior, MLP = mid left lobe posterior, ARA = apex right lobe anterior, ARP = apex right lobe posterior, ALA = apex left lobe anterior, ALP = apex left lobe posterior, TP = true positive, TN = true negative, FP = false negative.